Environmental Science Processes & Impacts

PAPER

View Article Online
View Journal | View Issue

Cite this: *Environ. Sci.: Processes Impacts*, 2025, **27**, 649

Identification of dissipation pathways for pharmaceuticals in soils – a modelling approach†

Matthias Boeckmann, *[a] Jan Siemens,[b] Benjamin Justus Heyde [c] and Christiane Zarfl[a]

Concentrations of pollutants like pharmaceuticals in soils typically decrease over time, though it often remains unclear whether this dissipation is caused by the transformation of the pollutant or a decreasing extractability. We developed a mathematical model that (1) explores the plausibility of different dissipation pathways, and (2) allows the quantification of concentration differences between aqueous soil extracts and soil solution. The model considers soil particles as uniform spheres, kinetic sorption towards an equilibrium (Freundlich model), and two dissipation pathways, *i.e.* irreversible transformation and mineralization (following 1st order kinetics) as well as the formation of non-extractable residues *via* intraparticle diffusion. Applying the model to 19 published datasets (eight pharmaceuticals, three soils) showed that intraparticle diffusion accounts for approximately two thirds of all simulated mass fluxes. Reversible formation of non-extractable residues could play a major role for dissipation, while irreversible transformation and mineralization cannot be excluded either based on the available datasets. The difference between concentrations in aqueous extracts and soil solution quantified by the model is below typical model and measurement uncertainties for most of the investigated pharmaceuticals. Larger differences might be linked to a positive ionic charge of the pollutant. The model helps in disentangling different dissipation pathways in soils and optimizing experiments elucidating the long-term fate of pollutants in soils.

Received 13th December 2024
Accepted 4th January 2025

DOI: 10.1039/d4em00777h

rsc.li/espi

Environmental significance

Antimicrobial resistance (AMR) poses a severe threat to public health and spreads, among others, also in soils that are subjected to inputs of antibiotic agents and other pharmaceuticals when fertilized with manure or irrigated with treated or untreated wastewater, which might (co-)select AMR. In order to assess the risk of AMR selection and development, it is crucial to quantify the bioavailable and bioaccessible antibiotic concentration over time and space. However, measuring this concentration in soils is challenging due to small pore water volumes and potential biases in soil extraction procedures. Using published data from soil incubation and batch experiments with various antibiotics, this study develops and applies a process-based mathematical model to quantify the extraction bias, evaluate the different dissipation pathways of antibiotics in soils and estimate the bioavailable antibiotic concentration. These results, combined with knowledge on microbial dynamics and AMR formation, provide a comprehensive assessment of the actual environmental risk posed by antibiotics in soils.

Introduction

Most of the thousands of chemical compounds we produce and use end up in soils or sediments, either through direct inputs, atmospheric deposition, flooding, irrigation or application of fertilizers or waste materials.[1,2] Observed concentrations of pollutants in soils typically decline over time following their input, a phenomenon that is termed "dissipation".[3,4] However, the mere observation of decreasing concentrations does not allow to distinguish between different processes that lead to a removal from the measurable fraction.[3,5,6] It thus often remains unclear whether the compound's dissipation is due to actual removal processes like degradation and mineralization, or due to sorption and other sequestration processes that lead to a decrease in the compound's accessibility. As a result, pollutants may still persist in soil but, technically, cannot be observed anymore with the currently available extraction methods and instruments.

Common extraction methods to measure pollutant concentrations in soils in the laboratory distinguish between easily extractable and residual fractions.[7,8] Nevertheless, any extraction

[a]Eberhard Karls University of Tübingen, Department of Geosciences, Schnarrenbergstraße 94-96, 72076 Tübingen, Germany. E-mail: matthias.boeckmann@uni-tuebingen.de

[b]Justus Liebig University Gießen, Institute of Soil Science and Soil Conservation, iFZ, Heinrich-Buff-Ring 26-32, 35392 Gießen, Germany

[c]Ruhr University Bochum, Institute of Geography, Unit Soil Sciences and Soil Ressources, Bochum, Germany

† Electronic supplementary information (ESI) available. See DOI: https://doi.org/10.1039/d4em00777h

method necessarily interferes with the quantity it aims to observe. Lesueur *et al.* 2008 showed that different extraction methods lead to different results.[9] While the dilution effect of changing the liquid-to-solid ratio in the soil during extraction can principally be factored out, this correction is complicated by the fact that a change in the liquid to solid ratio leads to a shift in the equilibrium distribution of the pollutant in the soil in favour of the aqueous phase. This potential shift in equilibrium and the potentially resulting extraction bias have hardly been studied systematically.[10–14] Since the fraction of pollutants dissolved in the aqueous phase is commonly regarded as the most mobile and biologically effective fraction, a bias in the estimates of aqueous phase concentrations hampers the assessment of risks associated with the occurrence of pollutants in soils.[15] One example is the comparison of concentrations of antibiotics in aqueous extracts of soils with minimum inhibitory concentrations (MICs) and minimum selective concentrations (MSCs) determined in laboratory incubation experiments in which microorganisms are exposed to antibiotics that are dissolved in an aqueous growth medium at well-defined concentrations.[16,17]

A process-based model could be able to simulate the extraction process, explore the extraction bias and either allow to correct for it or provide justification to neglect it. Some existing modelling approaches link sorption directly to physical processes under steady-state conditions, but are not designed to simulate time series that reflect the kinetics.[18,19] Existing dynamic models are able to simulate observed sorption time series, but are either not able to consider multiple conceptual substance fractions in agricultural soil differing in binding strength and accessibility (easily extractable – EAS, residual – RES, non-extractable – NER and the fraction resulting from transformation and mineralization – TM)[20–22] or are based on simple first-order kinetics without considering physical processes.[13,23,24] However, intraparticle diffusion was previously proposed as an important mechanism in sorption.[25] Hence, a model that can simulate multiple pollutant fractions differing in binding strength extractability and accessibility over time based on physical processes is still missing.

Therefore, the overarching objective of this study is to develop a mathematical model based on published data for antibiotics and other pharmaceuticals extracted from soils over time that distinguishes different dissipation pathways of pollutants in soils and quantifies their kinetics. The model explores pollutant sorption *via* intraparticle diffusion as a possible dissipation pathway in addition to transformation and formation of non-extractable residues. Since the model reflects conceptually the actual chemical fate processes and not, technically, the extraction steps, it helps to simulate undisturbed processes in comparison to simulated extraction fractions to quantify the discrepancy in the aqueous concentration introduced by the extraction method (extraction bias). Hence, by applying the model to measured extraction data on antibiotics in different soils this study aims to (1) identify and quantify the processes that lead to antibiotic dissipation in soil, and (2) quantify the extraction bias that occurs if the easily extracted pollutant concentration is considered equal to the actual dissolved concentration.

Methods

General procedure

In this study, the conceptual understanding of sorption, sequestration and transformation of pharmaceuticals in soils has been translated into respective mathematical models that are each based on a system of ordinary differential equations representing the physico-chemical processes that drive the substance fate in soils. Available data in the literature on sequential soil extractions of pharmaceuticals were used to identify relevant processes that allow a meaningful representation of the observations by comparing different model structures derived by including or excluding potential sorption and dissipation pathways. Model parameter values, *e.g.* kinetic rate constants, were deduced by fitting the model structures to the extraction data during the calibration procedure. A local and a global sensitivity analysis were run to quantify the impact of changes in parameter values on the model outcome. Mass flux rates were simulated to identify the main processes governing the fate of the pharmaceuticals.

Based on the model development and quantification, simulations were run to identify the extraction bias that might be induced by shifts in the liquid-to-solid ratio during soil extraction in the laboratory.

Underlying data

In total, 19 datasets of time series of extractions of eight pharmaceuticals from natural soils from Germany or Mexico from Sittig *et al.* 2012, Dalkmann *et al.* 2014 and Förster *et al.* 2009 (ref. 12–14) (Table 1) were used for this study. Confidence intervals of time series were not available for these datasets. However, the average relative standard deviation of replicate measurements was ~50% for Dalkmann *et al.* 2014 and ~20% for Förster *et al.* 2009. No standard deviations were provided in Sittig *et al.* 2012. For each of the datasets, natural soils (0–30 cm depth) had been collected from the Mezquital Valley, north of Mexico City (Dalkmann) or from Merzenhausen and Kaldenkirchen in western Germany (Sittig and Förster). The investigated soils cover a large range of soil properties like clay content or organic matter content (Table 2), and developed under humid temperate climate conditions[12,14] or tropical steppe climate.[13] Since all soils were used as cropland, the variation of soil pH was only moderate ranging from slightly alkaline to slightly acidic (Table 2). The general extraction procedure is briefly outlined here, more details can be found in the references of the datasets. While Förster *et al.* 2009 and Dalkmann *et al.* 2014 extracted soils that were incubated in the dark with water spiked with pollutants under constant temperature and moisture in the laboratory over 150 days[13] or 215 days,[14] the experiments by Sittig *et al.* 2012 were implemented in an end-over-end-shaker with a soil suspension for 60 days. In all experiments, at least an easily extractable fraction (EAS, following a mild extraction procedure with 10 mM $CaCl_2$) and a residual fraction (RES, from an extraction step with methanol, acetonitrile and phosphoric acid, partly combined with high temperature in a microwave oven) of the substances have been

Table 1 Chemical properties of substances for which time series datasets on soil extraction are available

Substance	Molecular weight [g mol^{-1}]	pK_a	Log K_{OW}	Investigated by
Bezafibrate	362 (ref. 26)	3.6 (ref. 27)	3.97 (ref. 27)	Dalkmann *et al.*,[13] 2014
Carbamazepine	236 (ref. 26)	13.9 (ref. 27)	2.77 (ref. 27)	Dalkmann *et al.*,[13] 2014
Ciprofloxacin	331 (ref. 26)	6.1, 8.6 (ref. 28)	0.28 (ref. 29)	Dalkmann *et al.*,[13] 2014
Diclofenac	296 (ref. 26)	4.2 (ref. 27)	4.06 (ref. 27)	Dalkmann *et al.*,[13] 2014
Naproxen	230 (ref. 26)	4.2 (ref. 30)	0.33 (ref. 31)	Dalkmann *et al.*,[13] 2014
Sulfadiazine	250 (ref. 26)	2.5, 6.5 (ref. 32)	−0.07 (ref. 33)	Sittig *et al.*,[12] 2012, Förster *et al.*,[14] 2009
Sulfamethoxazole	253 (ref. 26)	1.7, 5.6 (ref. 34)	0.89 (ref. 33)	Dalkmann *et al.*,[13] 2014
Trimethoprim	290 (ref. 26)	7.2 (ref. 35)	0.91 (ref. 29)	Dalkmann *et al.*,[13] 2014

Table 2 Properties of the natural soils used in the extraction experiments

Soil	pH	OC [%]	Sand [%]	Silt [%]	Clay [%]	Duration of experiment [day]	Reference
Leptosol, Vertisol, Phaeozem; Mezquital Valley, Mexico	6.8–7.5	0.95–2.8	6.7–41	40–47	12–54	150	Dalkmann *et al.*[13] 2014
Silty loam; Merzenhausen, Germany	7.0	0.97	4.3	82.9	12.8	60	Sittig *et al.*[12] 2012
Luvisol; Merzenhausen, Germany	6.3	1.2	6	78	16	215	Förster *et al.*[14] 2009
Cambisol; Kaldenkirchen, Germany	6.0	1	75	22	3	215	Förster *et al.*[14] 2009

extracted and chemically analysed for a period of 60–215 days for 6–10 time points.

For 6 out of the 19 datasets, also the non-extractable residues could be quantified because the authors were able to work with radioactively-labelled compounds,[12,14] and for 3 datasets transformation products of the pharmaceuticals were determined. The dataset from Förster *et al.* 2009 (ref. 14) contains concentration data on two transformation products, 4-hydroxysulfadiazine (OH-SDZ) and *N*-acetylsulfadiazine (Ac-SDZ).

Conceptual model

In the conceptual model, the soil matrix is assumed to be a homogeneously mixed compartment (in analogy to batch conditions of the underlying lab experiments) that consists of an aqueous and a solid phase. The solid phase is conceptualized as spherical particles of homogenous size and material, covered with at least a film of water. In order to account for the different extraction fractions of the investigated pharmaceuticals, the particles are conceptually discretized into different shells S_i. In general, the pharmaceuticals are assumed to distribute between the different phases and particle shells by considering (equilibrium) Freundlich sorption, intraparticle diffusion processes as well as transformation and mineralization. More details on the processes are given below. In relation to the data gained from the available extraction experiments, the water phase and the outermost shell S_1 are considered to correspond to the EAS fraction while all inner shells correspond either to the RES fraction or, towards the centre of the particle, the fraction of non-extractable residues (NER).

The following processes that link the pharmaceutical fate in and between the different fractions are considered in the conceptual model (equations are given below): sorption equilibrium between the compound concentration in the aqueous phase and the outermost shell of the particles is assumed to follow the Freundlich model. Transfer of the compound between these two phases is thus following the gradient towards Freundlich sorption equilibrium. Intraparticle diffusion determines the exchange of the compound between all inner shells of the particle, *i.e.* the EAS, the shells corresponding to the RES and the inner-most NER fractions. Although the amount of NER technically describes the amount of pollutant that cannot be extracted by common extraction methods, the NER-formation is assumed to be potentially fully reversible. An alternative model structure with irreversible NER formation was tested to check the plausibility of fully reversible NER formation. The transformation and mineralization pool (TM) represents the substance fraction resulting from biotic transformation from the EAS fraction following first order kinetics. Sittig *et al.* 2012 (ref. 12) excluded other, *i.e.* abiotic, degradation pathways based on the observation of radiolabelled sulfadiazine.

Model equations

Mass balances. The basic condition for all model simulations here that represent conditions in a closed system is the mass balance. Hence the total mass of the pharmaceutical is given by:

$$m_{tot} = (C_{EAS} + C_{RES} + C_{NER} + C_{TM}) \times M_{tot} \quad (1)$$

where m_{tot} [M] is the total mass of the compound, while C_{EAS} [M M^{-1}], C_{RES} [M M^{-1}], C_{NER} [M M^{-1}] and C_{TM} [M M^{-1}] are the compound concentrations relative to the total soil mass M_{tot} in the EAS, RES, NER and TM fraction, respectively. The total mass of EAS comprises the compound fraction that is dissolved in the aqueous phase and the compound fraction in the outermost shell of the particles:

$$m_{EAS} = C_{W,aq} \times V_{aq} + S_1 \times M_{S_1} \quad (2)$$

where $C_{W,aq}$ [ML^{-3}] is the concentration in the aqueous soil phase (porewater) per volume of water, S_1 [M M^{-1}] is the content

of the compound in the outermost shell S_1 per mass of sorbent, V_{aq} [L^3] is the porewater volume and M_{S_1} [M] is the mass of shell S_1. The concentration in the EAS fraction (C_{EAS} [M M^{-1}]) related to the total soil bulk mass is given as:

$$C_{EAS} = C_{W,aq} \times \frac{\theta}{\rho} + \frac{S_1 \times M_{S_1}}{M_{tot}} \quad (3)$$

where θ [L^3 L^{-3}] is the volumetric water content and ρ [ML^{-3}] is the dry soil bulk density. The volume and mass of all shells are defined as equal based on the assumption that all particles are homogeneous, *i.e.* have a constant density throughout the particle. Hence, the mass of an individual shell is defined as:

$$M_{S_i} = \frac{M_{tot}}{n_{shell}} \quad (4)$$

where M_{S_i} [M] is the mass of any shell and n_{shell} [−] is the total number of shells. Inserted in eqn (3), this leads to:

$$C_{EAS} = C_{W,aq} \times \frac{\theta}{\rho} + \frac{S_1}{n_{shell}} \quad (5)$$

since all concentration data from the literature are given in mass of compound per mass dry bulk soil [M M^{-1}], C_W in [M M^{-1}] is defined, for consistency reasons, as:

$$C_w = C_{W,aq} \times \frac{\theta}{\rho} \quad (6)$$

and used in all equations following from here on.

The concentrations of the RES-fraction, C_{RES} [M M^{-1}], and the NER fraction, C_{NER} [M M^{-1}], are defined as the average mass of the compound that has been distributed into all shells defined as RES or NER, respectively, in relation to the total dry bulk soil mass:

$$C_{RES} = \frac{1}{n_{shells}} \sum_{i=2}^{n_{RES}+1} S_i \quad (7)$$

$$C_{NER} = \frac{1}{n_{shells}} \sum_{i=n_{RES}+2}^{n_{RES}+1+n_{NER}} S_i \quad (8)$$

where n_{RES} [−] and n_{NER} [−] are the numbers of shells that are assigned to RES and NER, respectively. The numbers of shells that correspond to the RES and the NER fraction is not fixed in the model structure but is derived from the fitting results, conceptually, a characteristic of the soil, the extraction procedure and the compound, in combination.

Differential equations. The compound dynamics in the soil as reflected in the extraction data are described by the following reference set of ordinary (because of assuming homogeneous spatial conditions) differential equations. Equilibrium between the compound concentration in the water phase and the outer particle shell is described by the Freundlich model:

$$K_f \left(C_W \frac{\rho}{\theta}\right)^m \overset{eq.}{=} S_1 \quad (9)$$

where K_f [$M_{pollutant}^{-m+1}$ M_{soil}^{-1} L_{water}^{3-m}] is the Freundlich coefficient and m [−] is the Freundlich exponent. The change of concentration in the water phase C_W is driven by the equilibration towards the Freundlich sorption equilibrium (based on Wehrhan *et al.* 2007 (ref. 36)) and the dissipation into the TM fraction following first order kinetics:

$$\frac{dC_W}{dt} = -\alpha\left(K_f\left(C_w \frac{\rho}{\theta}\right)^m - S_1\right) - k_{TM} C_W \quad (10)$$

where α [T^{-1}] is the kinetic Freundlich sorption rate constant and k_{TM} [T^{-1}] is the rate constant for transformation and mineralization. The change of concentration in the S_1-shell is controlled by the equilibration towards the Freundlich sorption equilibrium with the aqueous phase and the exchange with the inner spheres *via* intraparticle diffusion:

$$\frac{1}{n_{shells}} \frac{dS_1}{dt} = \alpha\left(K_f\left(C_W \frac{\rho}{\theta}\right)^m - S_1\right) - d_1\left(S_1 - \frac{S_2}{\beta}\right) \quad (11)$$

where d_i [T^{-1}] is the diffusion rate constant of shell i and β [−] is a scaling factor for the transformation from EAS to RES. This parameter serves as a proxy indicator for representing the optimal number of shells and their distribution (shells assigned to EAS, RES and NER) since direct calibration of the number of shells is infeasible due to numerical constraints. d_i is defined as:

$$d_i = \frac{D}{\Delta r_i^2} \quad (12)$$

where D [L^2 T^{-1}] is the apparent diffusivity of the material and Δr_i [L] is the respective distance between shells, calculated by:

$$\Delta r_i = \frac{r_i + r_{i+1}}{2} - \frac{r_{i+1} + r_{i+2}}{2} \quad (13)$$

where r_i [L] is the outer radius of the respective shell i. Since all shells are defined with the same volume, the outer radii of the shells are defined as:

$$r_1 = r_{sphere} \quad (14)$$

$$r_i = \sqrt[3]{\frac{1}{2}\left(r_{i-1}^3 + r_{i+1}^3\right)} \quad (15)$$

$$r_{n_{shells}} = \sqrt[3]{\frac{3V}{4\pi n_{shells}}} \quad (16)$$

where r_{sphere} [L] is the radius of the whole sphere, V [L^3] is its volume and $r_{n_{shells}}$ is the radius of the innermost shell. Eqn (14)–(16) represent a nonlinear system of equations, which is solved numerically.

The concentration change in all inner shells is driven by intraparticle diffusion:

$$\frac{1}{n_{shells}} \frac{dS_2}{dt} = d_1(S_1 - S_2) - d_2\left(\frac{S_2}{\beta} - S_3\right) \quad (17)$$

All other shells except the innermost shell are defined as:

$$\frac{1}{n_{shells}} \frac{dS_i}{dt} = d_{i-1}(S_{i-1} - S_i) - d_i(S_i - S_{i+1}); 3 \le i < (n_{shells} - 1) \quad (18)$$

whereas the innermost shell is defined as:

$$\frac{1}{n_{shells}} \frac{dS_{n_{shells}}}{dt} = d_{n_{shells}-1}\left(S_{n_{shells}-1} - S_{n_{shells}}\right) \quad (19)$$

The transformed and mineralized compound concentration C_{TM} expressed relative to the soil mass is defined analogously to the TM-term in eqn (10) as formation out of the fraction in water following first-order kinetics:

$$\frac{C_{TM}}{dt} = k_{TM} C_W \tag{20}$$

Initial conditions. For setting the initial conditions of the differential equations, the total concentration of the pharmaceutical was calculated based on the first observations of EAS and RES. These first observations were taken at $t = 0.24d$. Hence the respective masses at $t = 0d$ were extrapolated. The initial masses of EAS and RES were then distributed among the different phases/shells according to the following three assumptions:

(1) The initial distribution of mass between C_w and S_1 is ambiguous, as both phases are represented by the EAS-fraction. Hence, the mass distribution between these phases is assumed to be approximately even. In the context of sorption, this leads to the Freundlich sorption equilibrium according to eqn (9).

(2) The concentration of all inner shells that are assigned to RES is assumed to be scaled by an empirical, dimensionless gradient factor g, which is determined during calibration:

$$S_i \times g = S_{i-1} \tag{21}$$

(3) NER and, if applicable, TM are assumed to be zero.

Initialization of parameter values

Each parameter was initially defined by a prior distribution function based on all knowledge to start the calibration procedure of fitting the model to the available data and deriving optimal parameter values. By this, the empirical distribution of the parameter values resembles the prior distribution of the parameters (Table S1†). Hence, the parameter values are not limited to an arbitrary range, as the continuous prior distribution function can be chosen to cover all physically possible values.

To sample from these prior distributions, normalized parameter values were drawn from a uniform distribution between zero and one.

$$\bar{\boldsymbol{x}} \sim \mathcal{U}_{(0,1)} \tag{22}$$

where $\bar{\boldsymbol{x}}$ is the normalized location vector in the parameter space and $\mathcal{U}_{(0,1)}$ is the uniform distribution ranging from zero to one. The absolute parameter value is defined as the inverse cumulative probability density function of the respective parameter:

$$\boldsymbol{x}_i = \Phi_i^{-1}(\bar{\boldsymbol{x}}_i) \tag{23}$$

where $\boldsymbol{x}_i$ is the absolute value of the respective parameter that is used for the model simulation, Φ_i^{-1} is the inverse cumulative probability density function of the respective parameter and i is the parameter index.

Model calibration

Model equations were fitted to the 19 sets of extraction time series to gain a set of optimum model parameter values for each combination of pharmaceutical compound and soil. The datasets from Dalkmann *et al.* 2014 contain information about sterile and non-sterile conditions (except the ciprofloxacin dataset) under otherwise identical conditions, and thus a calibration in two steps was applied. The datasets under sterile conditions were used for calibration of all parameters except the rate constant for transformation and mineralization k_{TM} which is, conceptually, set to zero. Based on these calibration results, the six corresponding datasets under non-sterile conditions were evaluated by fixing the derived parameter values from the datasets under sterile conditions, and calibrating k_{TM}. These six datasets were excluded from the sensitivity analysis since all parameters except k_{TM} are fixed. For all other datasets which have all been derived from experiments under non-sterile conditions, all parameters including k_{TM} were used for calibration simultaneously.

The root-mean-square error (RMSE) between the observed and simulated values was defined as the objective function for minimizing the deviation between data and model outcomes.

$$\mathrm{RMSE} = \sqrt{\frac{\sum_{i=1}^{n_d} \left(y_{i,sim} - y_{i,obs}\right)^2}{n_d}} \tag{24}$$

where n_d is the number of data points, $y_{i,obs}$ is the respective observed datapoint, $y_{i,sim}$ is the simulated value and i is the datapoint index. Data points for different fractions (EAS, RES) were considered as data points from the same data series. The simulated values were created by solving the differential equations numerically. The RMSE was minimized using the *surrogateopt* algorithm in MATLAB. The algorithm relies on a surrogate model based on a radial basis function to evaluate promising points in the parameter space faster than the process-based model. For model comparison and comparison between extraction experiments, the normalized root mean square error (NRMSE) was used:

$$\mathrm{NRMSE} = \frac{\mathrm{RMSE}}{\max(y_{obs}) - \min(y_{obs})} \tag{25}$$

Alternative model structures

The reference model structure represents one possible explanation for transfer pathways and sorption processes but needs to be compared to potential alternative model structures that might explain the underlying experimental data equally well or even better. Thus, two alternative model structures were tested in the frame of evaluating model uncertainty: (1) irreversible NER-formation from RES and (2) reversible NER-formation from RES. Details of these alternative models are described in the ESI.† In addition, existing model approaches described in the literature were also applied to the available extraction data, if suitable, and respective results compared to the developed reference model.[12,23,36]

Sensitivity analysis

A model is considered sensitive to parameters that have the strongest effect on the simulation results, in this case, the RMSE between observed and simulated pollutant concentrations in the different soil phases. Sensitivity analyses, which determine the sensitivity of the model to its

parameters, can be categorized as local and global. Local sensitivity determines the sensitivity of a model only for a specific location in the parameter space while the global sensitivity analysis determines the mean sensitivity over the whole parameter space.

In cases where models contain multiple parameters, the sensitivity of the models towards individual parameters often varies strongly. Parameters to which the model is sensitive are considered active parameters.

To account for global sensitivity, Constantine *et al.* 2014 (ref. 37) proposed the active subspace method.[37] Constantine *et al.* 2014 (ref. 37) defined an active subspace as the eigenvectors of the matrix E:[37]

$$E = \int \nabla f(\bar{x}) \otimes f(\bar{x})\, q(\bar{x}) \mathrm{d}x \quad (26)$$

$\otimes$ is the matrix product, q is the probability density function of the normalized parameters $\bar{x}$, and f is the objective function. The integration is performed by the Monte-Carlo-method:[38]

$$E \approx \frac{1}{M} \sum_{k=1}^{M} \nabla f(\bar{x}_k) \otimes \nabla f(\bar{x}_k) \quad (27)$$

M is the number of samples and is set to 10^4 and $\bar{x}_k$ are independently drawn normalized parameter vectors.

The global sensitivity was assessed by the metric of Constantine and Diaz:[39]

$$A_i = \sum_{j=i}^{n} \lambda_j {w_{i,j}}^2 \times 100 \quad (28)$$

where A_i is the activity score for parameter i, j is the eigenvector index, n is the number of eigenvalues (equal to the number of parameters), λ_j is the j-th eigenvalue and $w_{i,j}$ is the value for parameter i in the j-th eigenvector of the matrix E. The activity score is the square of the unit of the observation. Therefore, in this work, the square root of the activity score was used. To increase readability, the activity score is scaled to a range of 0 to 100.

The most common challenge in this approach is to reliably determine $\nabla f(\bar{x})$.[40] In this case, $f(\bar{x})$ is not an observation, but a simulation by the model. Hence, $f(\bar{x})$ is noise-free. Therefore, the finite-difference method poses a possibility to determine $\nabla f(\bar{x})$:

$$\nabla_i f(x) = \frac{f(x + \Delta x) - f(x)}{\Delta x} \quad (29)$$

In addition to the global sensitivity analysis a local sensitivity analysis was added around the fitted parameters. All calculations were implemented in MATLAB.[41]

Uncertainty analysis

The bootstrapping algorithm was used to determine the uncertainty of the calibration.[42] Efron and Tibshirani (1997) described bootstrapping as a smoothed version of cross-variance.[43] It is a method that involves multiple sub-datasets which are created by slight perturbations of the original dataset by resampling with replacement (bootstrap-samples). All resulting bootstrap-datasets were used for fitting, leading to different parameter sets for each bootstrap-sample. The resulting parameter sets formed a posterior distribution that were used as a measure of uncertainty for the determined parameter values (*e.g.*, 95% confidence interval).

Model application: estimation of the extraction bias

For the determination of the extraction bias, the pollutant concentration in the aqueous phase (C_W) was simulated with the parameters determined by the model calibration. All datasets describe extraction experiments for sorption to a clean soil and dissipation. Therefore, after spiking the soil with the respective pollutant, the pollutant mass in the soil water decreases over time (Fig. 1). With the beginning of the extraction step, the ratio of water to soil mass in the soil sample is increased. $C_{W,aq}$ (concentration per volume of water) is thus decreased by the same factor due to dilution. The simulation was then continued with the new soil to solution ratio for the typical duration of the extraction time (24 h). During this time, desorption takes place due to the deviation from the sorption equilibrium after the addition of the mild aqueous extractant. Hence, the simulation showed a sudden increase in pollutant mass in the water phase to return to the equilibrium concentration ratio between solids and liquid phase.

The extraction bias was calculated by simulating individual extractions at all time points sampled. Due to the shift in sorption equilibrium, the observed concentration values for the EAS fraction overestimate the pollutant mass in the water phase. This leads to an extraction bias, quantified as the NRMSE between the simulated pollutant concentration in the water phase and the simulated extracted concentration (Table S4†). Only observed time points were considered for the NRMSE. The correlation between calibrated parameter values and the extraction bias was tested using the two-sided Pearson and Spearman correlation coefficients as well as Kendall's τ.

Results and discussion

After calibration of parameters, the reference model structure describes the datasets reasonably well according to the indicators for goodness of fit (NRMSE < 0.3) and the visual agreement between model simulations and data (Fig. 1). Differences between datasets under sterile conditions (Fig. 1A and C) and non-sterile conditions (Fig. 1B and D) are small. The model quality of this reference model is comparable to the reference model by Zarfl *et al.* 2009 (ref. 23) (no significant difference between the NRMSEs, t-test, $p = 0.29$). Other published dynamic compartment models were not considered for comparison, because they do not account for all pollutant fractions included in the datasets used for our analysis (EAS, RES, NER and TM).[12,36]

Including the formation of TM under non-sterile conditions in the model structure leads to a different projected dynamic despite fixed parameter values for the formation of EAS, RES and NER. Remobilization of NER might become relevant over longer timescales in favour of the dissipation and actual removal from the soil by the formation of TM as indicated by a decrease of the simulated NER fraction (Fig. 1B and D). Remobilization is not reflected in the data and simulations for

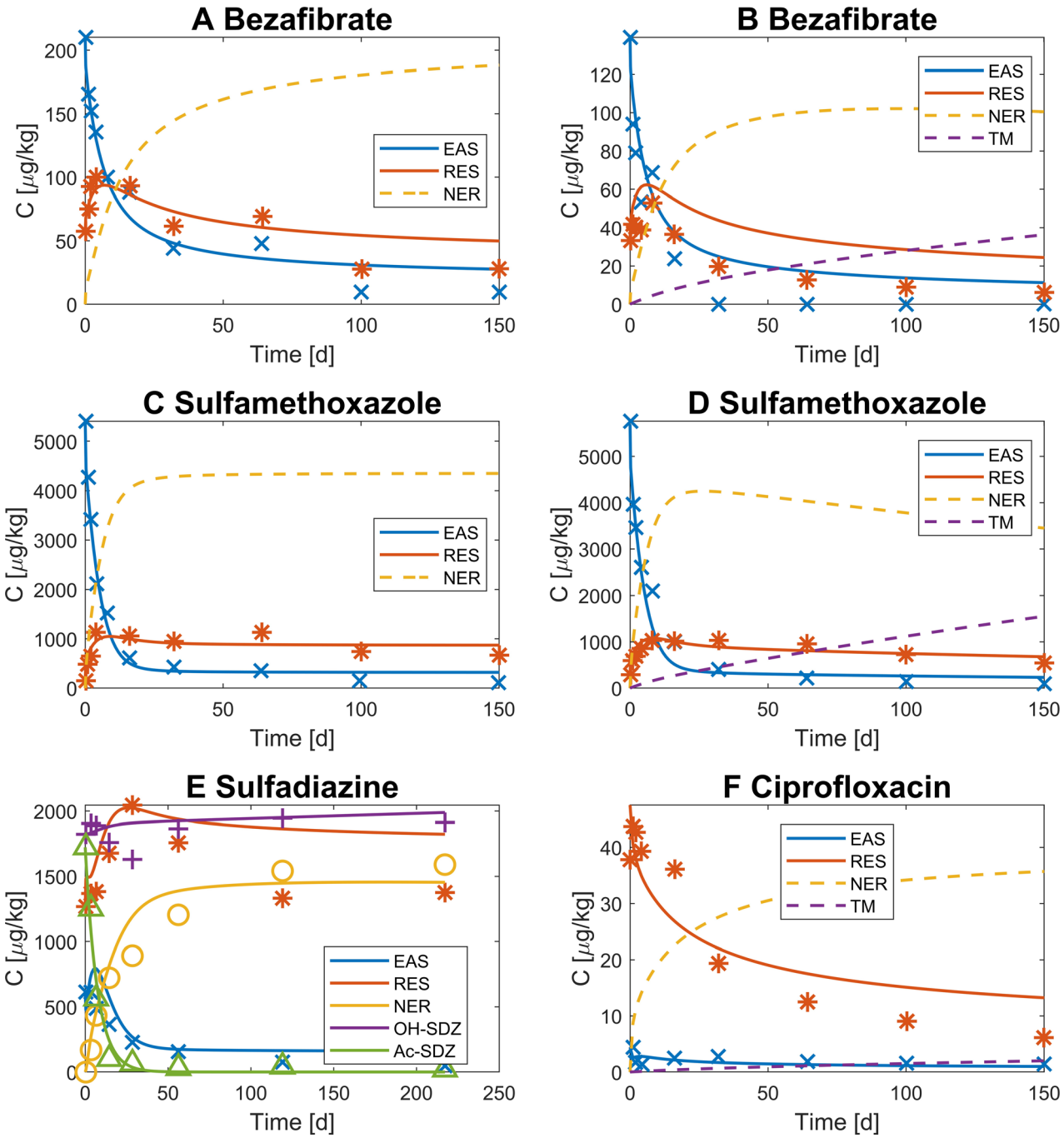

Fig. 1 Observed (markers) and simulated (lines) concentrations under sterile (A and C) and non-sterile conditions (B and D–F) for different pollutants in the easily extractable fraction EAS (blue), the residual fraction RES (red), the non-extractable fraction NER (yellow) and the transformed and mineralized fraction TM of the pollutant (purple). In sub-figure (E), the concentration of the transformation product of sulfadiazine, Ac-SDZ, is indicated in green. Dashed lines indicate simulation results for the substance fractions for which no data were available (in general TM and/or NER).

all compounds, *e.g.* sulfadiazine and ciprofloxacin, both under non-sterile conditions, over the observed timescale for which the simulated NER fraction reaches a plateau (Fig. 1E and F), suggesting that the reversibility of NER formation is a substance-specific behaviour if, in contrast to our assumption that NER was fully reversible, substance sequestration in soils is partially irreversible,[18] simulations longer than considered here might lead to an overestimation of long-term remobilization.

In the case of bezafibrate, the parameters from the dataset under sterile conditions lead to a slight overestimation of EAS and RES for the non-sterile dataset that could not be compensated by the formation of TM. This might be caused by an overestimation of the initial conditions and hence of the total mass of pharmaceutical in this case. *E.g.* an overestimation of 10% (within the experimental error) can cause a substantial overestimation of total mass in the system. In cases where a tailing of the

dissipation process is observed (due to a "balance" in long-term sequestration and desorption), the model was able to simulate this effect (Fig. 1A, C and D). Dissipation leads to a decrease in the observed pollutant mass in the EAS and RES fraction of all investigated compounds by an average of 60% by the end of the experiment (60–220 days). The NER and TM fractions increase analogously with the decrease in EAS and RES through dissipation. The relevance of the three main processes – Freundlich sorption, transformation and mineralization as well as intraparticle-diffusion – differs substantially between substances and presence or absence of microbial activity (see Table 3). For the first 40 days, Freundlich sorption and intraparticle diffusion contribute almost equally to the total average mass flux, while transformation and mineralization play only a minor role in the non-sterile datasets (set to zero for the sterile datasets). The mass fluxes of the respective processes were normalized to the number of elements within a process (*e.g.* shells in the particle, soil water, TM pool, *etc.*) to factor out an overestimation of the respective mass flux by transitions within the same process (*e.g.* diffusion between multiple shells). The relevance of Freundlich sorption decreases over time in favour of diffusion. Intraparticle diffusion is generally much slower to equilibrate due to the high number of particle shells. Therefore, its relative relevance is higher in later stages of the experiment, although total mass fluxes are orders of magnitude lower in these later stages of the experiment. Unlike sorption the formation of TM is irreversible. Hence, it only ceases when all pollutant mass is transformed and/or mineralized. Due to the low availability of pollutant mass in the water phase, this process is very slow. This leads to higher relative mass fluxes of TM in later stages of the experiment when sorption processes are close to equilibrium. The relevance of transformation and mineralization might be underestimated, since any amount of pollutant might be part of the Freundlich sorption and intraparticle diffusion process multiple times but can only once undergo the transition to the TM pool.

The role of the kinetic sorption processes in relation to their equilibrium state changes during the course of the experiment. Therefore, the simulated aqueous compound concentration (C_w) and the compound concentration averaged across all particle shells are compared to their respective equilibrium (Fig. 2). Please note that the sorption equilibrium (dashed lines in Fig. 2) changes gradually due to the irreversible formation of TM, which reduces the total available mass of pollutant over time and thus the absolute equilibrium concentrations. In the beginning of the experiment, concentrations differ substantially from the sorption equilibrium.

In the example shown in Fig. 2, the concentrations approach equilibrium of Freundlich sorption in the first half of the experiment. After this, sorption processes between the outer shell and the aqueous phase are almost in equilibrium and their sorption kinetics play only a minor role. The time required to reach Freundlich sorption equilibrium differs substantially between pharmaceuticals. Fast sorbing pharmaceuticals equilibrate almost instantly (*e.g.* trimethoprim, carbamazepine).

Estimation of the extraction bias

Based on the estimated extraction bias, the investigated pharmaceuticals can be divided into substances with high extraction bias ($NRMSE_{extract} \geq 0.47$) and those with low extraction bias ($NRMSE_{extract} \leq 0.28$) (see Fig. 3 for comparison). The categorization of a substance as having a "high extraction bias" corresponds to an overestimation of the soil water concentration of more than 40%. The substances with high extraction bias include ciprofloxacin, trimethoprim and carbamazepine. Ciprofloxacin and

Table 3 Relative mass fluxes of the respective processes normalized to the number of elements within that process and normalized to the reference soil mass of one kilogram (mean value, ranges in the line below). Only those pollutants are listed for which the average mass flux in the first forty days exceeds one percent of the total mass in the soil

	0–40 days				40–80 days			
Simulation time	Sorption [%]	TM [%]	Diffusion [%]	Mass flux [µg per day]	Sorption [%]	TM [%]	Diffusion [%]	Mass flux [µg per day]
Bezafibrate non-sterile	72	6	22	4.5	20	10	70	0.2
	69–74	3–13	17–25	3.8–5.6	4–32	7–11	60–89	0.1–0.2
Bezafibrate sterile	66	0	34	6.1	33	0	67	0.7
	50–75		25–50	4–8.4	23–57		43–77	0.6–1
Ciprofloxacin non-sterile	0.3	0	100	0.2	1	0	99	0.07
	0–9	0–0.1	91–100	0.1–1.6	0–22	0–0.2	78–100	0.04–0.1
Diclofenac non-sterile	13	5	80	23.5	1	3	96	0.04
	8–19	1–11	78–89	9.2–31.5	0–1	1–6	94–98	0.01–0.4
Diclofenac sterile	7	0	93	160	17	0	83	0
	0–28		72–100	50–200	0–95		5–100	0–0.5
Naproxen non-sterile	78	10	12	86	67	17	16	30
	77–78	10–11	12–13	82–94	67–67	17–18	16–16	30–33
Naproxen sterile	81	0	19	70	68	0	32	25
	25–84		16–75	26–160	54–76		24–46	18–34
Sulfamethoxazole non-sterile	49	1	50	303	4	13	83	4
	48–50	0–2	49–51	291–320	2–15	0–14	77–86	2–7
Sulfamethoxazole sterile	52	0	48	297	14	0	86	2
	3–62		38–97	257–500	6–65		35–94	0–4

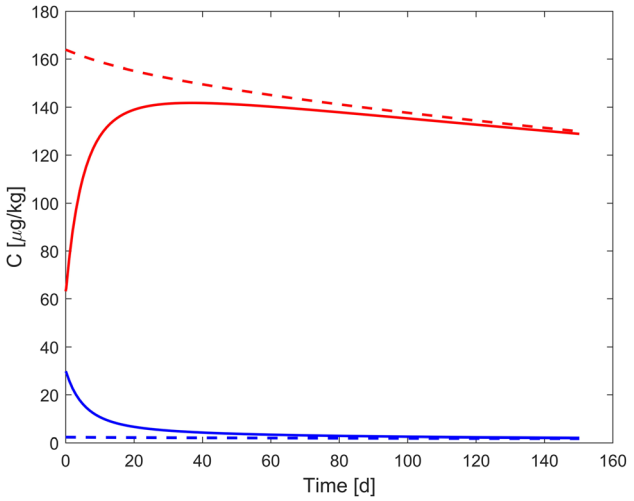

Fig. 2 Simulation of bezafibrate concentrations in the aqueous phase (C_W, blue) and averaged across all particle shells (red) in a non-sterile soil. Dashed lines indicate the equilibrium concentrations, based on the Freundlich-model, while solid lines indicate the simulation results with the calibrated model.

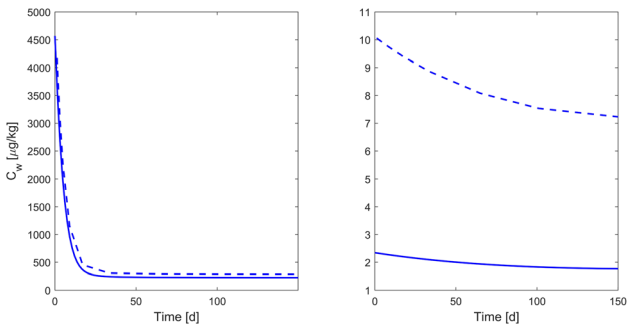

Fig. 3 Exemplary visualization of the simulated sulfamethoxazole (left) and trimethoprim (right) concentration under sterilized conditions in soil water (C_W) without extraction (solid blue) and as it would be observed in the extracted fraction (dashed blue).

trimethoprim are the only pharmaceuticals in the analysed dataset which have a positive charge at soil pH (Table S3†), so that cation exchange is a possible sorption process.[44–46] Cation exchange with Ca^{2+} added with the $CaCl_2$ extraction solution is a possible explanation for fast desorption that causes a high extraction bias. A previous study identified a correlation between sorption of trimethoprim and ciprofloxacin and cation exchange capacity.[44] Carbamazepine is the only substance with a neutral charge at soil pH, which is a possible reason for fast desorption that has also been described by other studies, especially from carbon rich substrate.[47,48]

Most calibrated parameters show little to no correlation to the extraction bias. Only the Freundlich exponent m shows a significant correlation (Table S2†). The correlation for the Freundlich exponent m is highest for the Pearson coefficient and much lower and not significant for Spearman and Kendall's τ. Kendall's τ is less susceptible to extreme values.[49] Hence, the correlation shown by the Pearson coefficient might be mostly based on the more extreme values for pharmaceuticals with high extraction bias.

Sensitivity and uncertainty analysis

Unlike a local sensitivity, the global sensitivity is a property of the model. It depends on the chosen prior parameter distribution but not on the calibrated parameter values. Since some parameter distributions are compound-specific, the sensitivity is not necessarily equal for all compounds, but is averaged over compounds that are simulated with the same combination of model and data source (Tables S5–S7†). For the model used for the sterile datasets from Dalkmann *et al.* 2014,[13] the RES and NER fractions are most sensitive to the apparent diffusivity D, since diffusion affects these fractions directly. EAS, which is only directly affected by Freundlich sorption, is most sensitive towards the Freundlich sorption rate parameter α and the Freundlich parameters K_f and m. Overall, out of all sorption parameters, the model is most sensitive to m, which can be explained by its exponential effect. K_f is the least sensitive sorption parameter, which is most likely outperformed by m, since both parameters describe the Freundlich equilibrium. EAS is, unlike all other fractions, moderately sensitive to the scaling factor β.

Unlike the sensitivity analysis for the model applied to the data from Dalkmann *et al.* 2014,[13] the sensitivity analysis for the model applied to the data from Sittig *et al.* 2012 (ref. 12) considers both dissipation pathways (TM and NER) (Table S6†). In this case, the mass fractions are most sensitive to the rate constant for transformation and mineralization k_{TM}. The sensitivity is highest for C_w and TM that are directly affected by the rate constant k_{TM}, and propagates to the other pollutant fractions. EAS and RES are most sensitive to the Freundlich sorption rate constant α and the Freundlich parameters K_f and m, due to Freundlich sorption affecting these quantities directly. NER is most sensitive to the apparent diffusivity D, which is the only parameter that controls the formation of NER. Unlike the rate constant k_{TM}, the sensitivity does not propagate to the other pollutant fractions. Most likely, this is caused by the availability of data about the NER fraction. This means that the amount of NER is fixed, while the amount of TM can only be estimated by the mass balance.

The sensitivity analysis for the model applied to the data of Förster *et al.* 2009 (ref. 14) is, in general, similar to the sensitivity results for the model related to the data from Sittig *et al.* 2012 (ref. 12) (Table S7†). Nevertheless, unlike all other datasets, transformation was observed in this dataset, so results regarding TM might be more reliable. In contrast to the sensitivity for the data from Sittig *et al.* 2012,[12] NER and RES are less sensitive to k_{TM}. This might be caused by additional information in the data on the transformation products, which is only the case in the datasets from Förster *et al.* 2009 (ref. 14) EAS is more sensitive towards the parameters describing transformation between OH-SDZ and Ac-SDZ than Freundlich sorption. Unlike for the other datasets, no quantity was sensitive to the apparent diffusivity D. Most likely, the kinetics of the formation of NER is more sensitive to the number of shells assigned to NER (see eqn (7) and (8)) than to the diffusive process described by D.

The confidence intervals of the determined parameters are relatively small for established processes like Freundlich sorption kinetic and equilibrium, while the confidence interval of

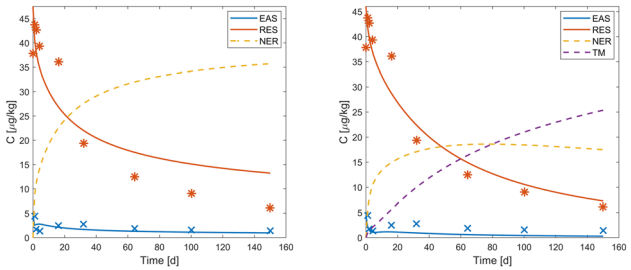

Fig. 4 Observed (markers) and simulated (lines) values of EAS (blue), RES (red), NER (yellow, dashed) and TM (purple, dashed) of ciprofloxacin. The left tile shows the NER-focused scenario. The right tile shows the TM-focused scenario. Note that the right tile necessarily indicates a better fit of the model to the data due to an additional parameter (k_{TM}) in the model structure available for calibration.

the apparent diffusivity D is much larger, since the exact nature of the diffusion process is less clear and might be more simplified than the Freundlich sorption (Tables S8–S10†).

Characterization of dissipation

Depending on the shell distribution, either the NER- or TM-dissipation pathway is dominant when both pathways are considered. The exact amount of NER and TM is known for the data from Sittig *et al.* 2012 (ref. 12) and Förster *et al.* 2009,[14] where NER was quantified experimentally (see Fig. S2 and S3†). However, the dataset from Dalkmann *et al.* 2014 (ref. 13) does not contain NER or TM data. Therefore, the shell distribution cannot be fitted in the same way as for the other two datasets. In the case where both, sterile and non-sterile, datasets were available, it was possible to determine the parameter k_{TM} for transformation and mineralization from the comparison of these two cases, assuming no transformation and mineralization under sterile conditions. In the case of ciprofloxacin, only data taken under non-sterile conditions was available. The model showed similarly good fits when considering the NER-pathway or the TM-pathway (see Fig. 4). This indicates that it is in general not possible to distinguish between NER and TM solely by applying the different model structures to extraction data without any knowledge about potential degradation products or inclusion of a sterile treatment.

Conclusions

The assessment of environmental risks associated with pollutants requires the estimation of "bioaccessible", "bioavailable" and mobile pollutants fractions in soils, which change over time, based on sound conceptual models. In this study, the abstraction of the soil as homogeneous spherical particles is one of several options to conceptualize the soil's solid phase. Diffusion to the centre of the particle as described in this model concept might, in reality, be reflected in similar mechanisms that cause hysteresis. *E.g.*, if pollutant mass diffused into the outer half (radius-wise) of the particle only and the apparent diffusivity was a quarter of the fitted value (due to the quadratic nature of diffusion over distance), the modelled observations would look similar, assuming that the number of, now smaller shells, stays the same. These mechanisms are indistinguishable from the chosen mechanisms from a modelling perspective. A differentiation between transformation and mineralization on the one hand and NER formation on the other hand requires either the complete experimental quantification of transformation products or the quantification of NER formation *e.g.* by means of isotope-labelled compounds, experiments under sterile and non-sterile conditions or longer observation times to observe possible desorption. Otherwise, the model cannot differentiate between these processes. Extended observation periods may also be considered to test the reversibility of NER formation. If the isolated determination of the individual simulated processes in experiments were possible, the uncertainties for the structure and parameters of the model could be decreased.

The estimated extraction bias was negligibly small for most of the pharmaceuticals that were investigated in the datasets we used. Hence, simple extractions with aqueous solutions allow a reasonable assessment of "bioaccessible", "bioavailable" or biologically effective concentrations of pharmaceuticals. The cases for which the estimation of "bioaccessible", "bioavailable" or "bioeffective" concentrations based on "mild", aqueous extracts might be challenging can probably be identified in advance based on the chemical properties of the observed compounds (*i.e.* ionic charge).

Data availability

No new data was created in this study. The used MATLAB-Code is available at: **https://www.github.com/Sigma-Librae/IPDSM**.

Author contributions

M. B., J. S. and C. Z. designed the research. M. B. created the model, performed analysis, and visualized graphics. C. Z., J. S. and B. J. H. substantially contributed to the interpretation of results. M. B. outlined the manuscript and all co-authors revised the work carefully. All authors have read and agreed to the published version of the manuscript.

Conflicts of interest

There are no conflicts to declare.

Acknowledgements

This work was supported by the Research Unit "Pollutant – Antibiotic Resistance–Pathogen Interactions in a Changing Wastewater Irrigation System" (PARES, FOR 5095), funded by the German Research Foundation (DFG, Project no. 431531292). We also acknowledge fiancial support from the Open Access Publishing Fund of the University of Tübingen. We thank Peter Grathwohl for his comments and insights.

References

1 J. I. Nieto-Juárez, R. A. Torres-Palma, A. M. Botero-Coy and F. Hernández, Pharmaceuticals and environmental risk

assessment in municipal wastewater treatment plants and rivers from Peru, *Environ. Int.*, 2021, **155**, 106674.
2 B. Gworek, M. Kijeńska, J. Wrzosek and M. Graniewska, Pharmaceuticals in the soil and plant environment: a review, *Water, Air, Soil Pollut.*, 2021, **232**, 145.
3 R. Kodešová, M. Kočárek, A. Klement, O. Golovko, O. Koba, M. Fér, A. Nikodem, L. Vondráčková, O. Jakšík and R. Grabic, An analysis of the dissipation of pharmaceuticals under thirteen different soil conditions, *Sci. Total Environ.*, 2016, **544**, 369–381.
4 M. Cycoń, A. Mrozik and Z. Piotrowska-Seget, Antibiotics in the soil environment—degradation and their impact on microbial activity and diversity, *Front. Microbiol.*, 2019, **10**, 338.
5 P. A. Blackwell, P. Kay and A. B. A. Boxall, The dissipation and transport of veterinary antibiotics in a sandy loam soil, *Chemosphere*, 2007, **67**, 292–299.
6 E. Pose-Juan, M. J. Sánchez-Martín, E. Herrero-Hernández and M. S. Rodríguez-Cruz, Application of mesotrione at different doses in an amended soil: Dissipation and effect on the soil microbial biomass and activity, *Sci. Total Environ.*, 2015, **536**, 31–38.
7 I. Rosendahl, J. Siemens, J. Groeneweg, E. Linzbach, V. Laabs, C. Herrmann, H. Vereecken and W. Amelung, Dissipation and sequestration of the veterinary antibiotic sulfadiazine and its metabolites under field conditions, *Environ. Sci. Technol.*, 2011, **45**, 5216–5222.
8 T. Müller, I. Rosendahl, A. Focks, J. Siemens, J. Klasmeier and M. Matthies, Short-term extractability of sulfadiazine after application to soils, *Environ. Pollut.*, 2013, **172**, 180–185.
9 C. Lesueur, M. Gartner, A. Mentler and M. Fuerhacker, Comparison of four extraction methods for the analysis of 24 pesticides in soil samples with gas chromatography–mass spectrometry and liquid chromatography–ion trap–mass spectrometry, *Talanta*, 2008, **75**, 284–293.
10 L. Cáceres-Jensen, J. Rodríguez-Becerra, C. Garrido, M. Escudey, L. Barrientos, J. Parra-Rivero, V. Domínguez-Vera and B. Loch-Arellano, Study of Sorption Kinetics and Sorption–Desorption Models to Assess the Transport Mechanisms of 2,4-Dichlorophenoxyacetic Acid on Volcanic Soils, *Int. J. Environ. Res. Public Health*, 2021, **18**, 6264.
11 R. Đurović-Pejčev, S. Radmanović, Z. P. Tomić, L. Kaluđerović and T. Đorđević, Characterization of the clomazone sorption process in four agricultural soils using different kinetic models, *Environ. Sci.:Processes Impacts*, 2023, **25**, 542–553.
12 S. Sittig, R. Kasteel, J. Groeneweg and H. Vereecken, Long-term sorption and sequestration dynamics of the antibiotic sulfadiazine: A batch study, *J. Environ. Qual.*, 2012, **41**, 1497–1506.
13 P. Dalkmann, C. Siebe, W. Amelung, M. Schloter and J. Siemens, Does long-term irrigation with untreated wastewater accelerate the dissipation of pharmaceuticals in soil?, *Environ. Sci. Technol.*, 2014, **48**, 4963–4970.
14 M. Förster, V. Laabs, M. Lamshöft, J. Groeneweg, S. Zühlke, M. Spiteller, M. Krauss, M. Kaupenjohann and W. Amelung, Sequestration of manure-applied sulfadiazine residues in soils, *Environ. Sci. Technol.*, 2009, **43**, 1824–1830.
15 J. Menz, J. Müller, O. Olsson and K. Kümmerer, Bioavailability of antibiotics at soil–water interfaces: A comparison of measured activities and equilibrium partitioning estimates, *Environ. Sci. Technol.*, 2018, **52**, 6555–6564.
16 I. C. Stanton, A. K. Murray, L. Zhang, J. Snape and W. H. Gaze, Evolution of antibiotic resistance at low antibiotic concentrations including selection below the minimal selective concentration, *Commun. Biol.*, 2020, **3**, 1–11.
17 D. Schuster, K. Axtmann, N. Holstein, C. Felder, A. Voigt, H. Färber, P. Ciorba, C. Szekat, A. Schallenberg, M. Böckmann, C. Zarfl, C. Neidhöfer, K. Smalla, M. Exner and G. Bierbaum, Antibiotic concentrations in raw hospital wastewater surpass minimal selective and minimum inhibitory concentrations of resistant Acinetobacter baylyi strains, *Environ. Microbiol.*, 2022, **24**, 5721–5733.
18 M. Sander, Y. Lu and J. J. Pignatello, A Thermodynamically Based Method to Quantify True Sorption Hysteresis, *J. Environ. Qual.*, 2005, **34**, 1063–1072.
19 M. Sander and J. J. Pignatello, Sorption irreversibility of 1,4-dichlorobenzene in two natural organic matter–rich geosorbents, *Environ. Toxicol. Chem.*, 2009, **28**, 447–457.
20 A. Wehrhan, T. Streck, J. Groeneweg, H. Vereecken and R. Kasteel, Long-Term Sorption and Desorption of Sulfadiazine in Soil: Experiments and Modeling, *J. Environ. Qual.*, 2010, **39**, 654–666.
21 K. Brimo, P. Garnier, S. Sun, J.-L. Bertrand-Krajewski, A. Cébron and S. Ouvrard, Using a Bayesian approach to improve and calibrate a dynamic model of polycyclic aromatic hydrocarbons degradation in an industrial contaminated soil, *Environ. Pollut.*, 2016, **215**, 27–37.
22 G. Lashermes, Y. Zhang, S. Houot, J. P. Steyer, D. Patureau, E. Barriuso and P. Garnier, Simulation of Organic Matter and Pollutant Evolution during Composting: The COP-Compost Model, *J. Environ. Qual.*, 2013, **42**, 361–372.
23 C. Zarfl, J. Klasmeier and M. Matthies, A conceptual model describing the fate of sulfadiazine and its metabolites observed in manure-amended soils, *Chemosphere*, 2009, **77**, 720–726.
24 A. Berez, F. Ayari, N. Abidi, G. Schäfer and M. Trabelsi-Ayadi, Adsorption-desorption processes of azo dye on natural bentonite: batch experiments and modelling, *Clay Miner.*, 2014, **49**, 747–763.
25 J. J. Pignatello and B. Xing, Mechanisms of Slow Sorption of Organic Chemicals to Natural Particles, *Environ. Sci. Technol.*, 1996, **30**, 1–11.
26 PubChem, PubChem, **https://pubchem.ncbi.nlm.nih.gov/**, accessed 9 August 2023.
27 K. Styszko, J. Szczurowski, N. Czuma, D. Makowska, M. Kistler and Ł. Uruski, Adsorptive removal of pharmaceuticals and personal care products from aqueous solutions by chemically treated fly ash, *Int. J. Environ. Sci. Technol.*, 2018, **15**, 493–506.

28 P. C. Sharma, A. Jain, S. Jain, R. Pahwa and M. S. Yar, Ciprofloxacin: review on developments in synthetic, analytical, and medicinal aspects, *J. Enzyme Inhib. Med. Chem.*, 2010, **25**, 577–589.
29 B. Halling-Sørensen, H.-C. H. Lützhøft, H. R. Andersen and F. Ingerslev, Environmental risk assessment of antibiotics: comparison of mecillinam, trimethoprim and ciprofloxacin, *J. Antimicrob. Chemother.*, 2000, **46**, 53–58.
30 M. Röhricht, J. Krisam, U. Weise, U. R. Kraus and R.-A. Düring, Elimination of carbamazepine, diclofenac and naproxen from treated wastewater by nanofiltration, *Clean:Soil, Air, Water*, 2009, **37**, 638–641.
31 F. Barbato, G. Caliendo, M. I. La Rotonda, C. Silipo, G. Toraldo and A. Vittoria, Distribution coefficients by curve fitting: Application to ionogenic nonsteroidal antiinflammatory drugs, *Quant. Struct.-Act. Relat.*, 1986, **5**, 88–95.
32 K. P. de Amorim, L. L. Romualdo and L. S. Andrade, Performance and kinetic-mechanistic aspects in the electrochemical degradation of sulfadiazine on boron-doped diamond electrode, *J. Braz. Chem. Soc.*, 2014, **25**, 1484–1492.
33 S. G. Machatha and S. H. Yalkowsky, Comparison of the octanol/water partition coefficients calculated by ClogP®, ACDlogP and KowWin® to experimentally determined values, *Int. J. Pharm.*, 2005, **294**, 185–192.
34 H. Lucida, J. E. Parkin and V. B. Sunderland, Kinetic study of the reaction of sulfamethoxazole and glucose under acidic conditions: I. Effect of pH and temperature, *Int. J. Pharm.*, 2000, **202**, 47–62.
35 O. Mikes and S. Trapp, Acute toxicity of the dissociating veterinary antibiotics trimethoprim to willow trees at varying pH, *Bull. Environ. Contam. Toxicol.*, 2010, **85**, 556–561.
36 A. Wehrhan, R. Kasteel, J. Simunek, J. Groeneweg and H. Vereecken, Transport of sulfadiazine in soil columns—experiments and modelling approaches, *J. Contam. Hydrol.*, 2007, **89**, 107–135.
37 P. G. Constantine, E. Dow and Q. Wang, Active subspace methods in theory and practice: Applications to Kriging surfaces, *SIAM J. Sci. Comput.*, 2014, **36**, A1500–A1524.
38 P. G. Constantine, C. Kent and T. Bui-Thanh, Accelerating Markov chain Monte Carlo with active subspaces, *SIAM J. Sci. Comput.*, 2016, **38**, A2779–A2805.
39 P. G. Constantine and P. Diaz, Global sensitivity metrics from active subspaces, *Reliab. Eng. Syst. Saf.*, 2017, **162**, 1–13.
40 D. Erdal and O. A. Cirpka, Global sensitivity analysis and adaptive stochastic sampling of a subsurface-flow model using active subspaces, *Hydrol. Earth Syst. Sci.*, 2019, **23**, 3787–3805.
41 MATLAB, *9.12.0.1884302 (R2022a)*, The MathWorks Inc., Natick, Massachusetts, 2022.
42 B. Efron, in *Breakthroughs in Statistics: Methodology and Distribution*, ed. S. Kotz and N. L. Johnson, Springer, New York, NY, 1992, pp. 569–593.
43 B. Efron and R. Tibshirani, Improvements on cross-validation: The 632+ bootstrap method, *J. Am. Stat. Assoc.*, 1997, **92**, 548–560.
44 L. Rodríguez-López, V. Santás-Miguel, R. Cela-Dablanca, A. Núñez-Delgado, E. Álvarez-Rodríguez, P. Pérez-Rodríguez and M. Arias-Estévez, Ciprofloxacin and trimethoprim adsorption/desorption in agricultural soils, *Int. J. Environ. Res. Public Health*, 2022, **19**, 8426.
45 F.-J. Peng, G.-G. Ying, Y.-S. Liu, H.-C. Su and L.-Y. He, Joint antibacterial activity of soil-adsorbed antibiotics trimethoprim and sulfamethazine, *Sci. Total Environ.*, 2015, **506–507**, 58–65.
46 A. Pasket, H. Zhang, Y. Wang, M. Krzmarzick, J. E. Gustafson and S. Deng, Clay content played a key role governing sorption of ciprofloxacin in soil, *Front. Soil Sci.*, 2022, **2**, 814924.
47 P. Oleszczuk, B. Pan and B. Xing, Adsorption and desorption of oxytetracycline and carbamazepine by multiwalled carbon nanotubes, *Environ. Sci. Technol.*, 2009, **43**, 9167–9173.
48 X. Ji, J. K. Challis, J. Cantin, A. S. Cardenas Perez, Y. Gong, J. P. Giesy and M. Brinkmann, A novel passive sampling and sequential extraction approach to investigate desorption kinetics of emerging organic contaminants at the sediment–water interface, *Water Res.*, 2022, **217**, 118455.
49 M. B. Abdullah, On a robust correlation coefficient, *J. R. Stat. Soc.*, 1990, **39**, 455–460.

